Optik - International Journal for Light and Electron Optics 182 (2019) 50–57

Contents lists available at ScienceDirect

Optik

journal homepage: www.elsevier.com/locate/ijleo

Original research article

Analysis on topology derivation of single-phase transformerless photovoltaic grid-connect inverters

Zhiling Liao*, Chenchen Cao, Diancheng Qiu

The School of Electrical and Information Engineering, Jiangsu University, Zhenjiang, China

ARTICLE INFO

Keywords:
PV system
Transformerless
Grid-Connected inverters
Leakage current
Topology derivation

ABSTRACT

Aiming at the leakage current problem of single-phase transformerless photovoltaic(PV) grid-connected inverters, the recent proposed topologies are classified and reviewed. These topologies are divided into half-bridge type and full-bridge type. The topology characteristics of transformerless PV inverter are analyzed. This paper presents some of transformerless PV inverter topologies and discusses the evolution laws among various topologies to clarify the interrelationship between them. Furthermore, according to the evolution laws, a new topology is proposed. Finally, Simulations and experiments compare leakage current suppression capability of the proposed topology, H5 topology and HERIC topology.

1. Introduction

Single phase transformerless PV grid-connected inverters have low cost, small size, and light weight, which can greatly improve efficiency [1]. However, since there is no isolation transformer, the PV panels and utility grid will have electrical connections through parasitic capacitors, filter inductors and filter capacitors in the circuit. Common mode (CM) leakage current is likely to increase greatly. In addition to increasing the grid current ripple and system loss, it will also cause safety issues [2]. According to German VDE 0126-1-1 standard [3], if the leakage current is over 300 mA, a break must be triggered within 0.3 s. In order to solve the problem of CM leakage currents, a large number of new topologies have been proposed by researchers.

In recent years, most of literatures on the PV inverters have focused on topology performance. There are few researches on topology derivation and evolution laws. Most of the topologies are relatively independent, lacking the interrelationship between topologies. Literatures [4,5] compare the topologies proposed in recent years from the aspects of device number, loss, CM voltage and power quality, but do not involve the evolution laws between topologies. In [6], some topologies are analyzed and classified according to different leakage current suppression methods, but the relationship between topologies is not discussed. Literature [7] only researched the evolution relationship between full-bridge type topologies, but does not involve half-bridge type topologies.

Based on the researches of above literatures, this paper analyzes single-phase transformerless PV grid-connected inverter topologies in recent years, and divides it into two categories: half-bridge type and full-bridge type. Furthermore, based on the evolution law, a new topology is derived. A brief comparison is made with H5 topology, HERIC topology and the proposed topology, which shows the advantages of the new topology. Finally, experiments confirm the good performance of the proposed topology.

* Corresponding author.
E-mail addresses: liaozhiling@ujs.edu.cn (Z. Liao), 2211707023@stmail.ujs.edu.cn (C. Cao), qiudiancheng@163.com (D. Qiu).

https://doi.org/10.1016/j.ijleo.2018.12.169
Received 17 December 2018; Accepted 29 December 2018

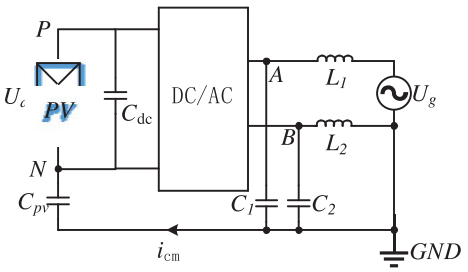

Fig. 1. CM equivalent model of single-phase PV inverter.

2. CM equivalent model of transformerless PV grid-connected inverter

The CM equivalent model of single-phase transformerless PV grid-connected inverter is given in [8], as shown in Fig. 1, where U_{dc} is the output voltage of the PV panel; C_{dc} is the DC-side capacitor; L_1 and L_2 are the filtering Inductance; C_{pv} is the parasitic capacitor of the PV panel to ground; C_1 and C_2 are parasitic capacitors of the bridge arm to ground.

The CM voltage U_{cm} is defined as follows:

$$U_{CM} = \frac{U_{AN} + U_{BN}}{2} + (U_{AN} - U_{BN})\frac{L_2 - L_1}{2(L_1 + L_2)} \tag{1}$$

where U_{AN} is the voltage between point A and point N, U_{BN} is the voltage between point B and point N.

The leakage current i_{cm} is defined as follows :

$$i_{cm} = C_{pv}\frac{dU_{CM}}{dt} \tag{2}$$

From (2), the leakage current is zero as long as the CM voltage U_{cm} is kept constant. The most used method is constructing new freewheeling loops or power transmission loops by changing the topology or modulation mode, so that the DC side and the AC side are disconnected, and the CM voltage is kept constant to suppress leakage current [8]. The key to new topologies is how to build new freewheeling loops and power transmission loops.

3. Half-bridge type transformerless PV grid-connected inverters

The single-phase half-bridge type PV inverter topology mainly includes two-level topologies and three-level topologies. The traditional two-level topology is shown in Fig. 2(a). There are only two switches and one inductor. However, the DC-link voltage utilization is low and voltage stress of switches are high. In addition, at the same switching frequency, its two-level output voltage harmonics are large, increasing the size and cost of filter [9].

In order to reduce the size of filter and voltage stress of the switches, the three-level neutral point clamped(3L-NPC) topology is proposed in [10], as shown in 2(b). The main disadvantage of 3L-NPC topology is that the switching losses between internal switches S_2, S_3 and external switches S_1, S_4 are not equal, which increases the difficulty of heat dissipation.

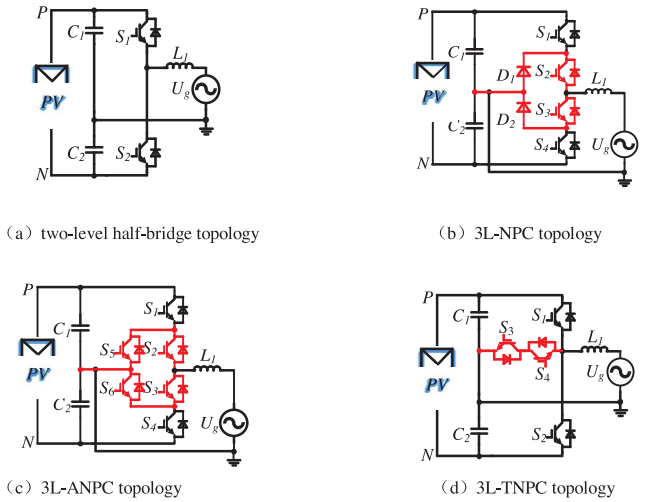

（a）two-level half-bridge topology

（b）3L-NPC topology

（c）3L-ANPC topology

（d）3L-TNPC topology

Fig. 2. Single-phase half bridge-type PV inverter.

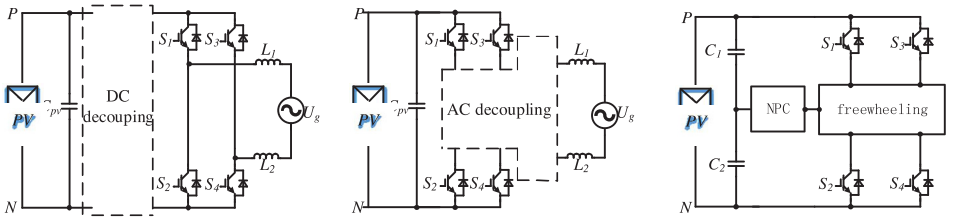

(a) DC decoupling topology (b) AC decoupling topology (c) topology with neutral point clamp

Fig. 3. single-phase full-bridge type PV inverters.

To balance the switching loss, literature [11] proposed a three-level active neutral point clamped(3L-ANPC) topology by replacing the passive switches by active switches, as shown in Fig. 2(c). However, there are two switches operating in any modes, which generates a large amount of conduction loss and reduces system efficiency.

In order to reduce the conduction loss, a three-level T-type neutral point clamped (3L-TNPC) topology is proposed in [12], as shown in Fig. 2(d). Two switches are inserted between the midpoint of the bridge arm. But the voltage stress of switches on the inverter bridge arm is larger than that of active clamp switches, which affects the heat dissipation design.

4. Full-bridge type transformerless PV grid-connected inverter

Bipolar SPWM can effectively suppress leakage current for traditional full-bridge inverter topologies. However, its two-level output voltage causes a large total harmonic distortion (THD), which requires a large filter. The output voltage of the unipolar SPWM is three-level and has low THD. But high leakage current is generated [13]. Therefore, a series of full-bridge improved topologies have been proposed, which can be divided into DC decoupling topology, AC decoupling topology and improved topology with neutral point clamp(NPC), as shown in Fig. 3.

4.1. DC decoupling transformerless inverters

H5 topology is proposed in [14], as shown in Fig. 4(a). A switch S_5 is added on the traditional full-bridge topology, and PV panels are disconnected from the grid by the turned-off of S_5, so that leakage current is suppressed. The advantage of the H5 topology is that it has fewer switches and lower cost. However, the switching frequency of S_5 is twice that of other switches. The switching loss of S_5 is greater than that of other switches, which increases the difficulty of heat dissipation.

To balance the loss of H5 topology, literature [15] proposed an improved topology: a switch S_6 is inserted corresponding to S_5, as shown in Fig. 4(b).The loss of S_5 is reduced by alternately operating of S_5 and S_6 during the freewheeling mode. Unfortunately, the disadvantage is that four switches are in the turn-on state during the power transmission mode. The conduction loss is high and the efficiency is reduced.

To reduce the conduction loss, another improved topology is proposed in [16]. Based on the H5 topology, a new switch is inserted to construct a new power transmission loop, as shown in Fig. 4(c). Current only passes through two switches during power transmission mode. Compared with the topology shown in Fig. 4(b), the efficiency is improved.

4.2. AC decoupling transformerless inverters

The topologies based on the DC decoupling have at least two switches conducting in the power transmission mode, and the conduction loss is large. On the basis of H5 improved topology II, a switch S_7 is inserted to construct a negative half-period power transmission loop. The entire power transmission mode always has only two switches, and the conduction loss is reduced. The switch S_5 is always in the turn-off state, so it can be removed from the topology, as shown in Fig. 5(a). Then HERIC topology is derived by circuit equivalent transformation, as shown in Fig. 5(b). Current will flow through the body diodes of switches in the freewheeling

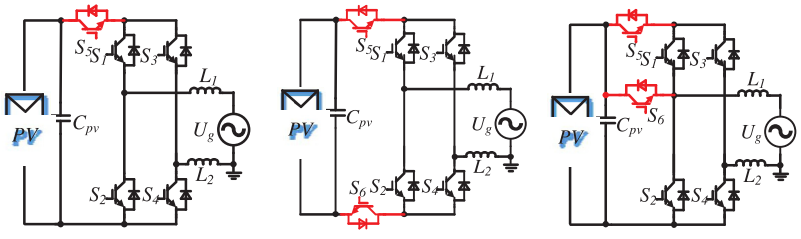

(a)H5 topology (b)H5 improved topology □ (c)H5 improved topology □

Fig. 4. Family of H5 topologies.

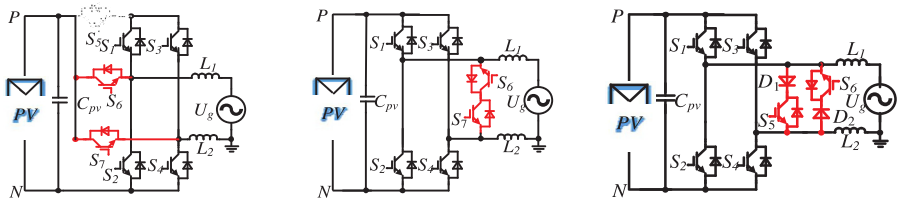

(a)transition of H5 to HERIC (b)HERIC □ (c)HERIC □

Fig. 5. DC decoupling–AC decoupling topology evolution.

loop. The body diodes are replaced by fast recovery diodes to reduce loss, as shown in the Fig. 5(c).

Literatures [17–20] proposed five transformation topologies of HERIC topology. In this paper, by analyzing these topologies, the evolution law is obtained: connecting equipotential points directly to change the power transmission loop and the freewheeling loop. S_1 and S_4 are turned on and S_2 and S_3 are turned off during the positive half-period power transmission mode in the HERIC II topology. Due to the presence of the D_2, no current flows through S_6 even if it is turned on. Therefore, multiple sets of equipotential points appear in the circuit. Connect one of them and then the circuit is equivalently transformed to obtain HERIC change 1 topology, as shown in Fig. 6(a). Similarly, connecting different equipotential points can obtain different change topologies, as shown in Fig. 6(b)–(e).

4.3. Improved topology with neutral point clamp

Due to the existence of various parasitic parameters in the circuit, the CM voltage does not remain constant. In order to better suppress the leakage current, literatures [21,22] proposed a variety of neutral point clamp structures, and CM voltage can be clamped to half of the dc bus voltage, as shown in Fig. 7. Different clamp structure can be combined with different topologies to achieve new topologies.

5. Summary of topological evolution

From the above topology derivation analysis, the following topological evolution laws can be obtained:

(1) Changing the power transmission loops or freewheeling loops is reflected in the derivation of H5 topological family. To reduce the conduction loss during power transmission mode, new power transmission loops or freewheeling loops can be constructed. Different loops can derive different topologies.
(2) Replacing passive diodes with active switches is reflected in the derivation of the 3L-ANPC topology. Replacing the diodes with IGBTs or MOSFETs can actively control the circuit to form a different loop, and a series of new topologies can be evolved.
(3) Connecting the equipotential point directly is reflected in the derivation of the HERIC topological family. When the circuit is running, multiple equipotential points appear. Connect two or more equipotential points directly, and then a series of new

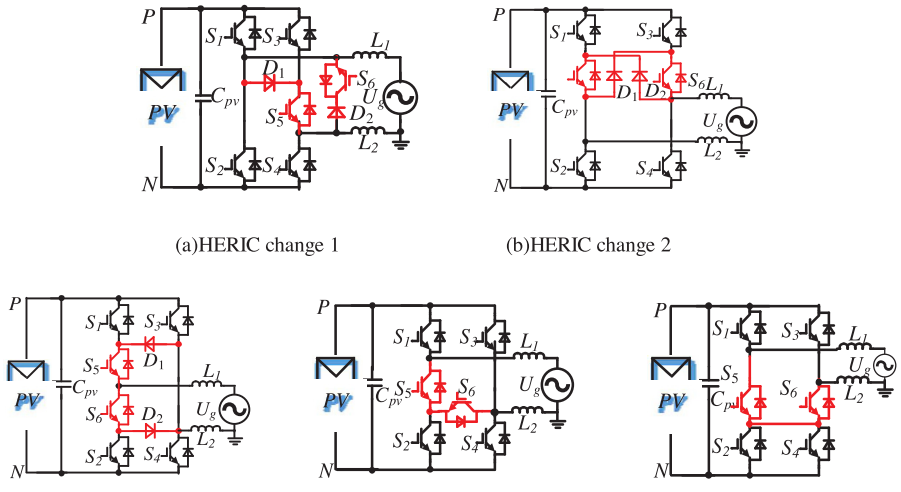

(a)HERIC change 1 (b)HERIC change 2

(c)HERIC change 3 (d)HERIC change 4 (e)HERIC change 5

Fig. 6. Family of HERIC topologies.

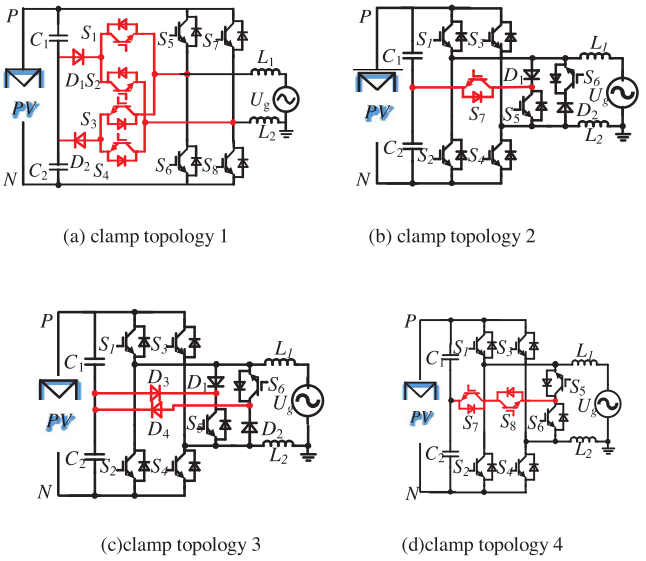

Fig. 7. Full-bridge type topologies with neutral-point- clamped structure.

topologies can be evolved through circuit equivalent transformation.

(4) Adding neutral point clamp structure is reflected in the derivation of clamp topologies. The CM voltage of the freewheeling loop is clamped to half of the DC bus. Combining different clamp structures with different topologies can constitute different new topologies.

6. Evolutionary derivation of a new topology

In order to further prove the evolution laws, the same new topology is derived in two different ways by using the evolution laws, as shown in Fig. 8.

The first way uses the evolution law(1) and (4). The switches S_5 and S_6 of HERIC change 4 operate at the switching frequency during freewheeling mode, and the switching loss is large. Two switches can be added to form a new freewheeling loop, so that S_5 and S_6 operate only in a half-period to reduce the switching loss. Adding a set of neutral point clamp structures to form a new topology. The second way uses the evolutionary law(2) and (4). First, the diodes D_1 and D_2 in the HERIC change 3 are replaced by active switches. By controlling active switches, new freewheeling loops can be constructed. Add a set of neutral point clamp structures to form a new topology. Through the above derivation process, the correctness of evolution law can be further proved.

The working mode of new topology is shown in Fig. 9. In the active mode of positive half-period, the DC side power is transmitted to the AC side through the switches S_1, S_4, and S_5. $U_{AN} = U_{PV}$, $U_{BN} = 0$ and the CM voltage $Ucm = (Udc + 0)/2 = Udc/2$.

In the freewheeling mode of positive half-period, the inductor current flows through S_8, D_2, D_1, S_5 and S_5, S_7. $U_{AN} = 0.5U_{PV}$, $U_{BN} = 0.5U_{PV}$ and the CM voltage $Ucm = (Udc + 0)/2 = Udc/2$.

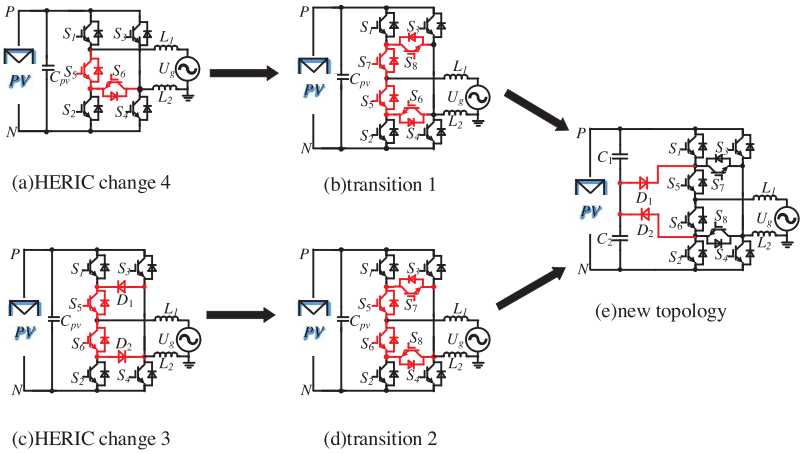

Fig. 8. Evolution process of the new topology.

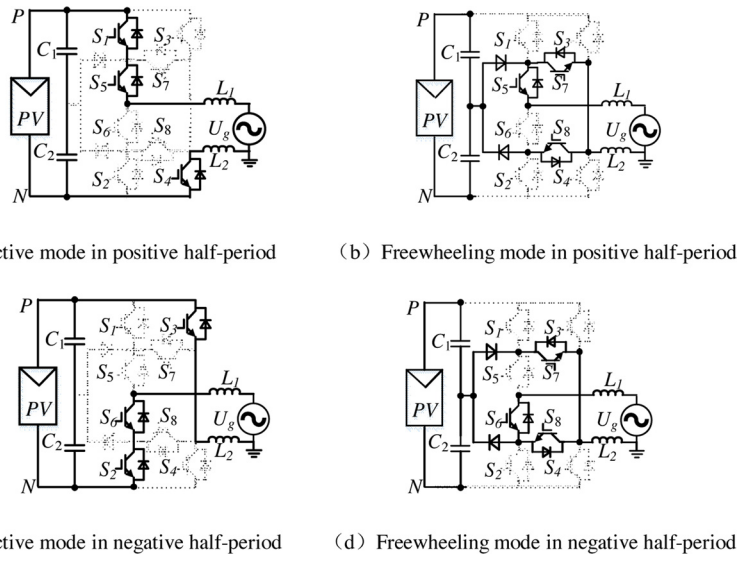

（a）Active mode in positive half-period （b）Freewheeling mode in positive half-period

（c）Active mode in negative half-period （d）Freewheeling mode in negative half-period

Fig. 9. Equivalent circuits of operation modes.

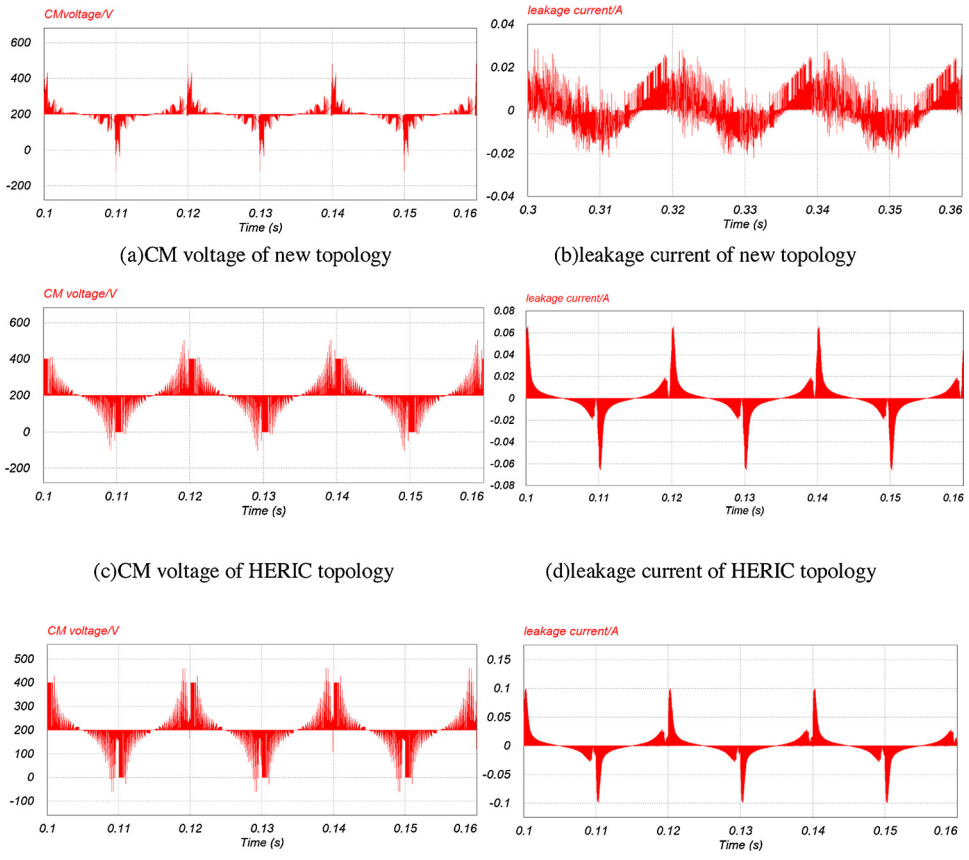

(a)CM voltage of new topology (b)leakage current of new topology

(c)CM voltage of HERIC topology (d)leakage current of HERIC topology

(e)CM voltage of H5 topology (f)leakage current of H5 topology

Fig. 10. Simulation results.

Negative half-period working mode is similar to positive half-period. CM voltage remains constant throughout the operating mode. So, leakage current can be suppressed.

The same device parameters and control strategy are used to build simulation model of the new topology, H5 and HERIC, as shown in Fig. 10.As a result, the leakage current of the new topology is only 20 mA, which is better than H5 topology and HERIC

Table 1
Simulation and experiment parameters.

parameter	value
Output power	1kW
Input voltage	DC400V
Grid voltage	AC220V
Grid frequency	50Hz
Switching frequency	20kHz
Parasitic capacitor	75nF
Input capacitor	100μF
Filter inductor	2mH

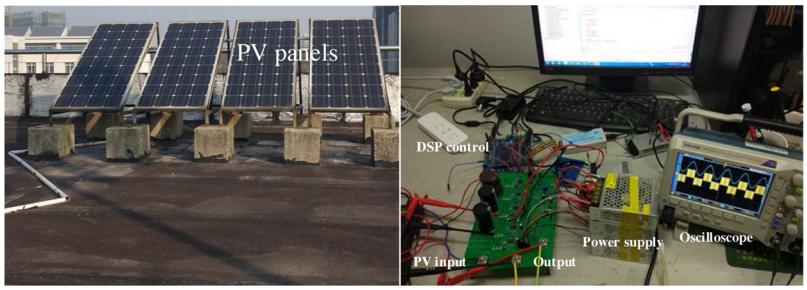

Fig. 11. Experimental Prototype.

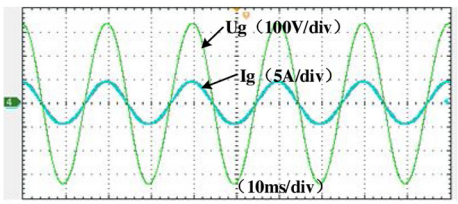

(a)grid voltage and current

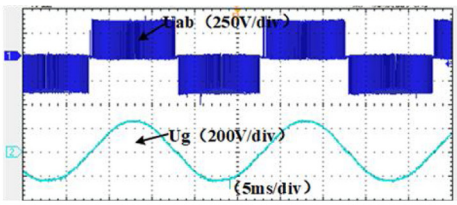

(b)output voltage and grid voltage

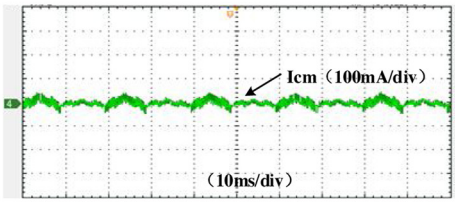

(c)leakage current

Fig. 12. Experiment results.

topology. The main simulation parameters are shown in Table 1. The experiment prototype is shown in Fig. 11. Experiments confirm the good performance of the proposed topology, as shown in Fig. 12.The total harmonic distortion(THD) of the grid-connected current is only 2.4% and the leakage current is only 20 mA.

7. Conclusion

(1) The characteristics of single-phase transformerless PV grid-connected inverters are summarized, and evolutionary derivation and classification are carried out.
(2) Four topological evolution laws are summarized from the topology evolution process, which proves that there is a close relationship between the topologies.
(3) A new topology is derived by using the evolution laws. It is verified by simulations and experiments that the new topology has good performance.
(4) The proposed topology evolution law can be used to better understand the existing topology, and provides a reference for the

subsequent new topology.

Author contributions

Chenchen Cao conceived and designed the study; Chenchen Cao and Diancheng Qiu performed the experiments; Zhiling Liao analyzed the results; Zhiling Liao and Chenchen Cao wrote the paper.

Conflicts of interest

The authors declare no conflicts of interest.

Acknowledgment

This work is financially supported by the Priority Academic Program Development of Jiangsu Higher Education Institutions (PAPD).

References

[1] Zeng Yangbin, Li Hong, Zhen Qionglin, et al., Research on the topological similarity and evolution law of single-phase photovoltaic non-isolated bridge-type inverters[J], Proceed. CSEE 37 (22) (2017) 6681–6690 (in Chinese).
[2] Wu Xuezhi, Yin jingyuan, Yang jie, et al., A novel single-phase transformerless photovoltaic grid-connected inverter[J], Power Syst. Technol. 37 (10) (2013) 2712–2718 (in Chinese).
[3] Automatic disconnection device between a generator and the public low-voltage grid, DIN VDE V 0126-1-1, 2006.
[4] K.S.F. Tan, J.H. Lee, H.C. Moon, et al., Modulation technique for single-phase transformerless photovoltaic inverters with reactive power capability[J], IEEE Trans. Ind. Electron. 64 (9) (2017) 6989–6999.
[5] Y.P. Siwakoti, F. Blaabjerg, Common-ground-type transformerless inverters for single-phase solar photovoltaic systems[J], IEEE Trans. Ind. Electron. 65 (3) (2018) 2100–2111.
[6] K.S.F. Tan, N.A. Rahim, W.P. Hew, et al., Comparison and analysis of single-phase transformerless grid-connected PV inverters[J], IEEE Trans. Power Electron. 29 (10) (2014) 5358–5369.
[7] Liao Zhiling, Cui Xiaochen, Xiong Yingjie, et al., A review of leakage current suppression techniques for transformerless photovoltaic grid-connected inverter[J], Electrical Meas. Instrum. 52 (22) (2015) 100–107 (in Chinese).
[8] Xiao Huafeng, Xie Shaojun, Chen Wenming, et al., Study on leakage current model for transformerless photovoltaic grid-connected inverter[J], Proceed. CSEE 30 (18) (2010) 9–14 (in Chinese).
[9] R. González, E. Gubía, J. López, L. Marroyo, Transformerless single-phase multilevel-based photovoltaic inverter[J], IEEE Trans. Ind. Electron. 55 (7) (2008) 2694–2702.
[10] J. Rodríguez, J.S. Lai, F.Z. Peng, Multilevel inverters: a survey of topologies, controls and applications[J], IEEE Trans. Ind. Electron. 49 (4) (2002) 724–738.
[11] T. Bruckner, S. Bernet, H. Guldner, The active NPC converter and its loss-balancing control[J], IEEE Trans. Ind. Electron. 52 (3) (2005) 855–867.
[12] S. Kouro, et al., Recent advances and industrial applications of multilevel converters[J], IEEE Trans. Ind. Electron. 57 (8) (2010) 2553–2580.
[13] A. Kadam, A. Shukla, A multilevel transformerless inverter employing ground connection between PV negative terminal and grid neutral point[J], IEEE Trans. Ind. Electron. 64 (11) (2017) 8897–8907.
[14] M. Victor, K. Greizer, and A. Bremicker. Method of converting a direct current voltage from a source of direct current voltage, more specifically from a photovoltaic source of direct current voltage, into a alternating current voltage. U.S. Patent 2005 028 6281 A1, Apr. 23, 1998.
[15] B. Yang, W. Li, Y. Gu, W. Cui, X. He, Improved transformerless inverter with common-mode leakage current elimination for a photovoltaic grid-connected power system[J], IEEE Trans. Power Electron. 27 (2) (2012) 752–762.
[16] G. San, H. Qi, J. Wu, X. Guo, A new three-level six-switch topology for transformerless photovoltaic systems, Proc. IPEMC, (2012), pp. 63–166.
[17] B. Ji, J. Wang, J. Zhao, High-efficiency single-phase transformerless PV H6 inverter with hybrid modulation method[J], IEEE Trans. Power Electron. 5 (60) (2013) 2104–2115.
[18] W. Yu, J. Lai, H. Qian, C. Hutchens, High-efficiency MOSFET inverter with H6-type configuration for photovoltaic nonisolated ac-module applications[J], IEEE Trans. Power Electron. 26 (4) (2011) 1253–1260.
[19] W. Cui, B. Yang, Y. Zhao, et al., IEEEA Novel Single-Phase Transformerless Grid-Connected Inverter[C]// Conference of the IEEE Industrial Electronics Society2011, A Novel Single-Phase Transformerless Grid-Connected Inverter[C]// Conference of the IEEE Industrial Electronics Society (2011).
[20] L. Zhang, K. Sun, Y. Xing, M. Xing, H6 transformerless full-bridge PV grid-tied inverters[J], IEEE Trans. Power Electron. 29 (3) (2014) 1229–1238.
[21] W. Li, Y. Gu, H. Luo, et al., Topology review and derivation methodology of single-phase transformerless photovoltaic inverters for leakage current suppression [J], IEEE Trans. Ind. Electron. 62 (7) (2015) 4537–4551.
[22] Xiao Huafeng, Yang Chen, Xie Shaojun, NPC three-level grid-connected inverter with leakage current suppression [J], Proceed. CSEE 30 (33) (2010) 23–29 (in Chinese).